AD-A200 955

RADC-TR-88-162
Final Technical Report
July 1988

III-V COMPOUNDS TRACE ELEMENT PROFILE ANALYSIS USING LASER ASSISTED SPECTROSCOPY

Aerodyne Research, Inc.

A. Freedman, K. McCurdy and C. Stinespring

DTIC
ELECTE
DEC 0 5 1988
S D
E

ROME AIR DEVELOPMENT CENTER
Air Force Systems Command
Griffiss Air Force Base, NY 13441-5700

88 12 5 066

This report has been reviewed by the RADC Public Affairs Division (PA) and is releasable to the National Technical Information Service (NTIS). At NTIS it will be releasable to the general public, icnluding foreign nations.

RADC-TR-88-162 has been reviewed and is approved for publication.

APPROVED: *David W. Weyburne*

DAVID W. WEYBURNE
Project Engineer

APPROVED: *Harold Roth*

HAROLD ROTH
Director of Solid State Sciences

FOR THE COMMANDER: *John A. Ritz*

JOHN A. RITZ
Directorate of Plans & Programs

If your address has changed or if you wish to be removed from the RADC mailing list, of it the addressee is no longer employed by your organization, please notify RADC (ESME) Hanscom AFB MA 01731-5000. This will assist us in maintaining a current mailing list.

Do not return copies of this report unless contractual obligations or notice on a specific document requires that it be returned.

REPORT DOCUMENTATION PAGE

Form Approved
OMB No. 0704-0188

1a. REPORT SECURITY CLASSIFICATION UNCLASSIFIED		1b. RESTRICTIVE MARKINGS N/A			
2a. SECURITY CLASSIFICATION AUTHORITY N/A		3. DISTRIBUTION/AVAILABILITY OF REPORT Approved for public release; distribution unlimited.			
2b. DECLASSIFICATION/DOWNGRADING SCHEDULE N/A					
4. PERFORMING ORGANIZATION REPORT NUMBER(S) ARI-RR-594		5. MONITORING ORGANIZATION REPORT NUMBER(S) RADC-TR-88-162			
6a. NAME OF PERFORMING ORGANIZATION Aerodyne Research, Inc.	6b. OFFICE SYMBOL (If applicable)	7a. NAME OF MONITORING ORGANIZATION Rome Air Development Center (ESME)			
6c. ADDRESS (City, State, and ZIP Code) 45 Manning Road Billerica MA 01821-3976		7b. ADDRESS (City, State, and ZIP Code) Hanscom AFB MA 01731-5000			
8a. NAME OF FUNDING/SPONSORING ORGANIZATION Rome Air Development Center	8b. OFFICE SYMBOL (If applicable) ESME	9 PROCUREMENT INSTRUMENT IDENTIFICATION NUMBER F19628-86-C-0142			
8c. ADDRESS (City, State, and ZIP Code) Hanscom AFB MA 01731-5000		10. SOURCE OF FUNDING NUMBERS			
		PROGRAM ELEMENT NO 65502F	PROJECT NO. 3005	TASK NO RA	WORK UNIT ACCESSION NO. 47

11. TITLE (Include Security Classification)
III-V COMPOUNDS TRACE ELEMENT PROFILE ANALYSIS USING LASER ASSISTED SPECTROSCOPY

12. PERSONAL AUTHOR(S)
A. Freedman, K. McCurdy and C. Stinespring

13a. TYPE OF REPORT Final	13b. TIME COVERED FROM Aug 86 TO Feb 87	14. DATE OF REPORT (Year, Month, Day) July 1988	15. PAGE COUNT 40

16. SUPPLEMENTARY NOTATION
N/A

17.	COSATI CODES		18. SUBJECT TERMS (Continue on reverse if necessary and identify by block number)
FIELD	GROUP	SUB-GROUP	Profile Analysis of Semiconductors
20	04		Laser Induced Fluorescence
14	02		Laser Ablation

19. ABSTRACT (Continue on reverse if necessary and identify by block number)

A microprobe analysis technique which has the potential for quantitative measurements of surface and bulk concentration as well as depth profiles has been investigated. This technique is termed Profile Analysis using Laser Assisted Spectroscopy (PALAS) and uses one pulsed laser to desorb or vaporize a controlled volume of the sample and a second pulsed laser to induce fluorescence in the desorbed species. The intensity of the laser induced fluorescence (LIF) provides a quantitative measure of the desorbed atom species concentration, while the energy density of the vaporizing laser controls the sampling depth. The requisite lateral resolution is provided by focusing the vaporizing laser. The purpose of the Phase I project was to demonstrate the feasibility of PALAS by making measurements of impurity and dopant concentrations in GaAs, which is a III-V material of interest to the Air Force and other defense agencies.

The system did not perform as well as anticipated. A number of deficiencies with the

20. DISTRIBUTION/AVAILABILITY OF ABSTRACT ☒ UNCLASSIFIED/UNLIMITED ☐ SAME AS RPT ☐ DTIC USERS	21. ABSTRACT SECURITY CLASSIFICATION UNCLASSIFIED	
22a. NAME OF RESPONSIBLE INDIVIDUAL David W. Weyburne	22b. TELEPHONE (Include Area Code) (617) 377-4015	22c. OFFICE SYMBOL RADC (ESME)

DD Form 1473, JUN 86 — Previous editions are obsolete.

machine as constructed were noted. In the light discrimination system, filters were not narrow enough and not effective enough at blocking out the broadband emissions. Two other problems, stray light scattering and slow vacuum pumping, were identified as machine dependent limitations. Finally, it was noted that the laser ablation step was dependent on the material being ablated. Thus, depth profiling of multilayered structures would be difficult with this system.

TABLE OF CONTENTS

i

1.0 INTRODUCTION

1.1 Motivation

Dopant and impurity concentrations in III-V and other semiconductor compounds must be precisely controlled, and in general, one is concerned not only with the bulk concentrations of these species but also with their surface and depth distribution or profile. Secondary ion mass spectrometry (SIMS), presently one of the most common diagnostics for such analyses, is subject to severe limitations.[1-4] Among these are problems in mass discrimination, quantification, and ultimate sensitivity. One example of the mass discrimination problem is the difficulty encountered in distinguishing between the Si_2 and Fe mass peaks at m/e= 56. Both silicon and iron are important trace species in III-V compounds whose concentrations must be precisely measured. Quantification problems in SIMS arise because of uncertainties in sputter ion yield and matrix effects, while limitations in sensitivity are due to the fact that the detected ions represent a very small fraction of the sputtered species.

A microprobe analysis technique which has the potential for quantitative measurements of surface and bulk concentration as well as depth profiles has been investigated. This technique is termed Profile Analysis using Laser Assisted Spectroscopy (PALAS) and uses one pulsed laser to desorb or vaporize a controlled volume of the sample and a second pulsed laser to induce fluorescence in the desorbed species. The intensity of the laser induced fluorescence (LIF) provides a quantitative measure of the desorbed atom species concentration, while the energy density of the vaporizing laser controls the sampling depth. The requisite lateral resolution is provided by focusing the vaporizing laser. The purpose of the Phase I project was to demonstrate the feasibility of PALAS by making measurements of impurity and dopant concentrations in GaAs, which is a III-V material of interest to the Air Force and other defense agencies.

1-1

PALAS, Profile Analysis using Laser Assisted Spectroscopy, is a variation
of the pump-probe technique which has been so valuable in analyzing gas phase
systems.[5-6] The concept involves using two lasers, one to perturb the system
to a transient condition and the second to measure the changes that have taken
place. In this variation, a pulsed laser vaporizes a surface monolayer (or
more if desired) of a desired material and the second laser induces
fluorescence in the atomic species that are formed. Specificity is provided
by the uniquely narrow linewidths of atomic transitions and sensitivity by the
concomitant large absorption strengths. Induced fluorescence detection has
been utilized for detection of both atomic and molecular species under many
circumstances.[7]

We note that this two laser approach contains other advantages. First,
the use of a pulsed laser to vaporize the surface allows one to accurately
control the depth of the probe. Recent work indicates that vaporization rate
is substrate dependent, but simple calibration experiments can be performed.
Lasers can be focused very accurately to provide high spatial resolution and
an entire chip can be scanned by rastering in order to provide information as
to doping or impurity level homogeneity. Unlike mass spectrometric
techniques, PALAS does not require an ultra-high vacuum apparatus thus
allowing in situ diagnostic measurements at a much lower cost.

1.2 Technical Background

Atomic spectroscopic transitions offer themselves as uniquely specific
and sensitive markers of the presence of elements at high dilution. Tables of
these transitions with their attendant line strengths are well known[8-9] and
one can calculate both the line width and absorption cross section by the
following equations:[10]

$$\Delta \nu = 7.162 \times 10^{-7} \, \nu_o \, (T/M)^{1/2} \tag{1}$$

$$\sigma_o = \frac{1.284 \times 10^{-12}}{\Delta \nu} A \frac{g_n}{g_m} \lambda^2 \tag{2}$$

where $\Delta\nu$ is the Doppler broadened linewidth in cm^{-1}, T the gas temperature, M the element atomic weight, σ_0 the absorption cross section at line center in cm^2, A the Einstein coefficient for spontaneous radiation in sec^{-1}, $g_{n,m}$ the degeneracies of the upper and lower states involved in the transition, and λ the transition wavelength in microns.

In order to calculate σ_0 and eventually the sensitivity, we must make several assumptions about how the measurement is performed. First, the vaporization laser is focused to a 10 μm spot with sufficient power to vaporize 5 monolayers (~20 Å) of the substrate. A reasonable time after the first laser pulse (depending on the vaporization dynamics and cessation of initial fluorescence), the probe laser is pulsed, inducing fluorescence in the vaporized atomic species. This fluorescence is collected by appropriate optics and sensed by a photomultiplier tube, whose signal is sent to a data acquisition system.

We therefore set the cell pressure at 10^{-4} torr which is low enough to ensure that the transition linewidth is indeed Doppler broadened and not pressure broadened. If the probe laser is pulsed at a point 10 microseconds after the initial pump, the plume will have expanded to a volume of ~1 cm^3 with a number density of approximately 10^{10} cm^{-3} (assuming a monolayer density of 10^{15} cm^{-2}). Table 1 lists the absorption cross sections of transitions in elements of interest (Si, Fe Ga, As, Al, Sn, etc.) for wavelengths easily accessible to pulsed dye lasers. It is important to note that even for the weakest transition (Fe), a modest-sized, narrow bandwidth nitrogen laser pumped dye laser has enough intensity to saturate the transition:

$$I_0 \sigma_0 \gg 1$$

where I_0 is the laser intensity in photons cm^{-2}. In this limit, the induced fluorescence photon yield, N, can be calculated:

$$N = n_0 \frac{g_n}{g_n + g_m} \quad photons/pulse \tag{3}$$

Table 1 - PALAS Sensitivity[a]

Element	Wavelength A°	Cross Section $(x10^{16} cm^2)$	Sensitivity (parts per million)
Fe	3860	4,400	2.5
Si	2514	12,000	0.6
Ga	4033	28,000	0.4
As	1973	13,000	0.8
Hg	2537	8,100	0.9
Cd	2288	204,000	0.04
Al	3944	11,700	0.1
Sn	2863	41,000	0.2
Cr	4290	13,000	0.7
Zn	2139	169,000	0.04
B	2497	11,000	1.5
Na	5890	130,000	0.06
K	7665	219,000	0.04
In	4102	43,000	0.2
Mn	4033	9,200	1.2

[a] Sensitivity estimated according to model presented in text.

where n_o is the element number density per cm^3 and it is assumed that the dye laser spatially overlaps the plume. The actual signal voltage is related to this by:

$$S = N \ F_o RC_o GW^{-1} \qquad (4)$$

where C_o is the optical collection efficiency, G is the photomultiplier tube gain, R is the value of the termination resistance, W is the acquisition time (usually set equal to A^{-1}), and F_o converts electron flow to current. Typically, C_o is 10^{-3}, $G = 10^7$, and $R = 50$ ohms. In the case of indium, for instance, we calculate that a concentration of 1 part per million will produce a 5 mV signal. Given the present data acquisition capabilities in our laboratory, we can conservatively detect a 1 mV pulse with signal to noise of one, yielding a detection capability of 200 parts per billion. Detection limits for other elements are presented in Table 1. It should be stressed that these estimates will vary with the precise application of the technique.

2.0 EXPERIMENTAL

Figure 1 provides a simplified schematic of the apparatus which is comprised of a vacuum cell, excimer laser, nitrogen pumped dye laser, and data acquisition system. The vacuum cell, a six way stainless steel cross of 4 inch diameter (MDC), is evacuated using a mechanical rotary pump to 1 torr and then to 10^{-4} torr using a liquid nitrogen cooled sorption pump (Huntington) which minimizes hydrocarbon contamination. All optical windows (Suprasil) are mounted on the system using O-ring seals except for the Brewster-angle mounted windows for the dye laser, which are epoxied (using Torr-Seal) onto their sidearms.

The sample was vaporized using an excimer laser (Model 2420, Questek) operated at 248 nm (K^rF) for all the experiments reported here with a repetition rate of 10 Hz. The laser output was directed through a limiting aperture (1 cm diameter) using dielectric coated mirrors and partially focussed at the sample using a 100 centimeter focal length (nominal) Suprasil lens. The unstable resonator optics on the laser, which reduces the near-field beam divergence to less than a tenth of a milliradian, allows for a well defined beam size which, at the sample, was measured to be oval with dimensions of 0.3 by 0.9 mm.

The sample was expoxied onto a silicon wafer which itself was mounted on a magnetically coupled rotary-linear motion feedthrough. This allowed for positioning of the sample with respect to the probe laser. The probe laser was a nitrogen laser pumped dye laser (Molectron UV14/DL14-P System) which provided 200 µJ pulses at 10 Hz in the blue wavelength region. The laser beam was transported to the apparatus by a fiber optic whose image was refocused, collimated, and polarized using several lenses and a UV polarizing sheet
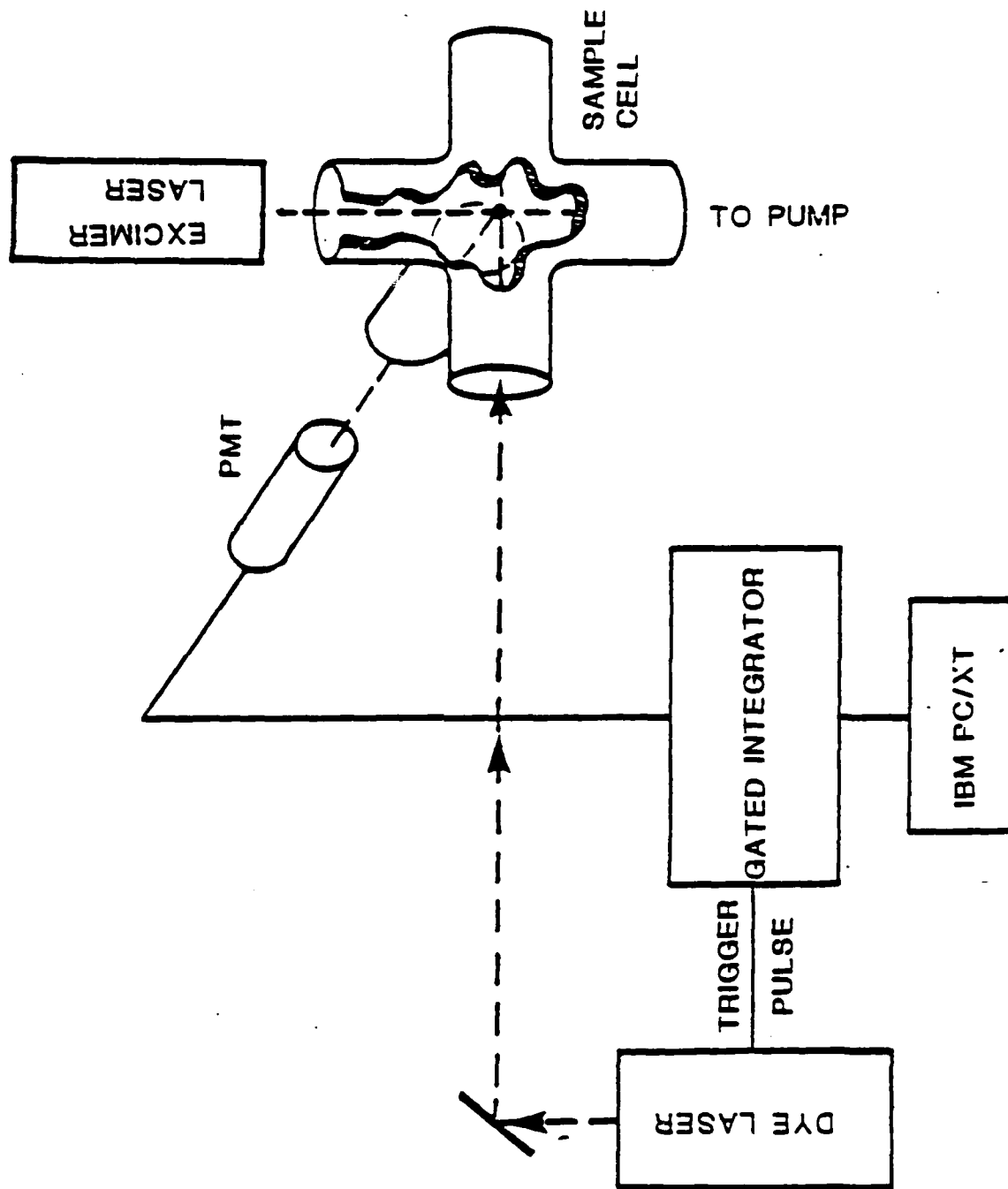
PALAS APPARATUS

Figure 1. Schematic of PALAS Apparatus

(Polacoat), so as to produce a ribbon shaped beam (~3 x 10 mm) parallel to the sample surface and orthogonal to the vaporization beam. The beam entered the vacuum cell through Brewster-angle windows so as to minimize light scattering.

The induced fluorescence was imaged by a quartz lens and focused through an interference filter (10 nm FWHM) onto a photomultiplier tube (Hamamatsu R212 UH) which was a high gain, low dark current variant of a standard 1P28 tube. The tube was mounted in an RFI shielded housing (Pacific Precision Instruments). The output of the PMT was routed to a preamplier (Ortec) and subsequently to a gated integrator (Stanford Research Systems) whose output was processed by an IBM PC/XT computer with an analog-digital converter board (Data Translation 2818). The timing sequence between the vaporization and probe lasers and the data acquisition system was controlled by a home-built[11] instrument using digital delay boards (Evans Associates) with 10 nsec resolution.

3.0 RESULTS

3.1 Pure Fe Foil

In order to assess the system performance, induced fluorescence from iron atoms which had been vaporized from iron foil was detected. Figure 2 presents an excitation spectrum obtained by scanning the wavelength of the probe laser (under computer control) and recording the fluorescence signal. Note that two peaks have been obtained—one (at 3859.91Å) from induced fluorescence from the ground electronic state and the other (at 3856.37Å) induced fluorescence from a low-lying excited electronic state 416 cm^{-1} (.052 eV) higher in energy. The spectral width reflects instrumental broadening of the laser linewidth of 0.1 Å (FWHM). The relative peak heights of the two transitions allows one to calculate an approximate plume temperature in the limit that such a description is applicable. The relative concentrations of the two states (n_1, n_2) are related to the observed signals (S_1, S_2) by the ratio of σ, the relative absorption cross section of the transition starting in each state.

$$\frac{n_1}{n_2} = \frac{S_1 \sigma_2}{S_2 \sigma_1}$$

The temperature, T, is defined by

$$\frac{n_2}{n_1} = \frac{g_2}{g_1} \exp(-\Delta E_o/RT)$$

where g is the degeneracy of the state, E_o is the term energy of the state, and R is the gas constant. Table 2 provides the relevant values of σ, g, and E_o. The temperature derived from this measurement is approximately 2400K, somewhat below the boiling point of iron (3023K), indicating that collisionally induced cooling has occurred in the plume.
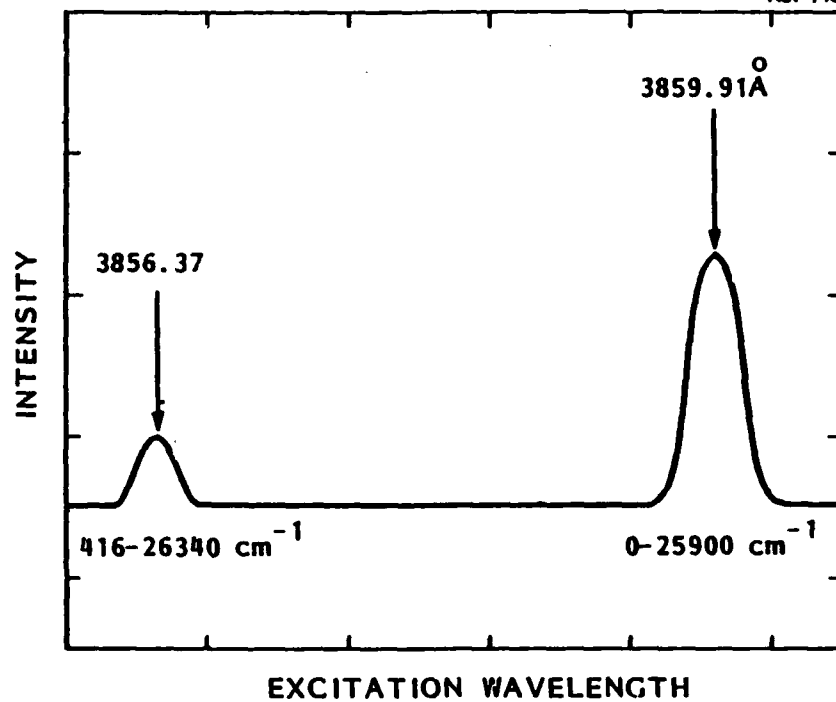
3-1

IRON INDUCED FLUORESCENCE

A87-140

Figure 2. Excitation Spectrum of Sample Vaporized From Iron Foil

Table 2. Low Lying Iron Atomic Transitions

Transition	σ	g	E_o(ev)
$0 \rightarrow 25900$ cm^{-1} $^5D_4 \leftarrow {}^5D_4$	1.0	7	0
$416 \rightarrow 26340$ cm $^5D_3 \leftarrow {}^5D_2$	0.3	9	0.052

Another check on the system was performed by measuring the apparent lifetime of the iron fluorescence from the ground state at 3859.91 Å. Previous studies have shown that signal non-linearities can result at short time delays due to collisional effects and/or high optical depth[13]. The apparent lifetime is straightforward measure of plume conditions. The lifetime was measured by setting the dye laser at a 15 μsec delay after the vaporization laser and delaying the detection system with respect to the dye laser. The results are shown in Figure 3. The delay between the two lasers was chosen so as to minimize problems from optically dense plumes where radiation trapping can interfere with the interpretation of the results. The recorded value of 110 nsec (over two lifetimes) compares favorably with a literature value of 100 nsec.[8]

We also wanted to show that our initial assumption that the transition could be saturated - i.e., insensitive to probe laser power - was correct. In this study, the probe laser was delayed 44 μsec after the vaporization laser (0.5 J cm^{-2}) and the signal measured as a function of the probe laser intensity by using neutral density filters to attenuate the beam. Figure 4 presents the results. At high attenuation, the signal is proportional to laser intensity as expected. As the intensity reaches the unattenuated value, the signal flattens out indicating that saturation is indeed starting to occur.

The next set of experiments investigated the nature of the iron plume itself. The first question that needed to be answered was whether there was a laser fluence threshold for producing gaseous iron atoms. Figure 5 presents results of changing the vaporization laser fluence (energy per unit area) at a
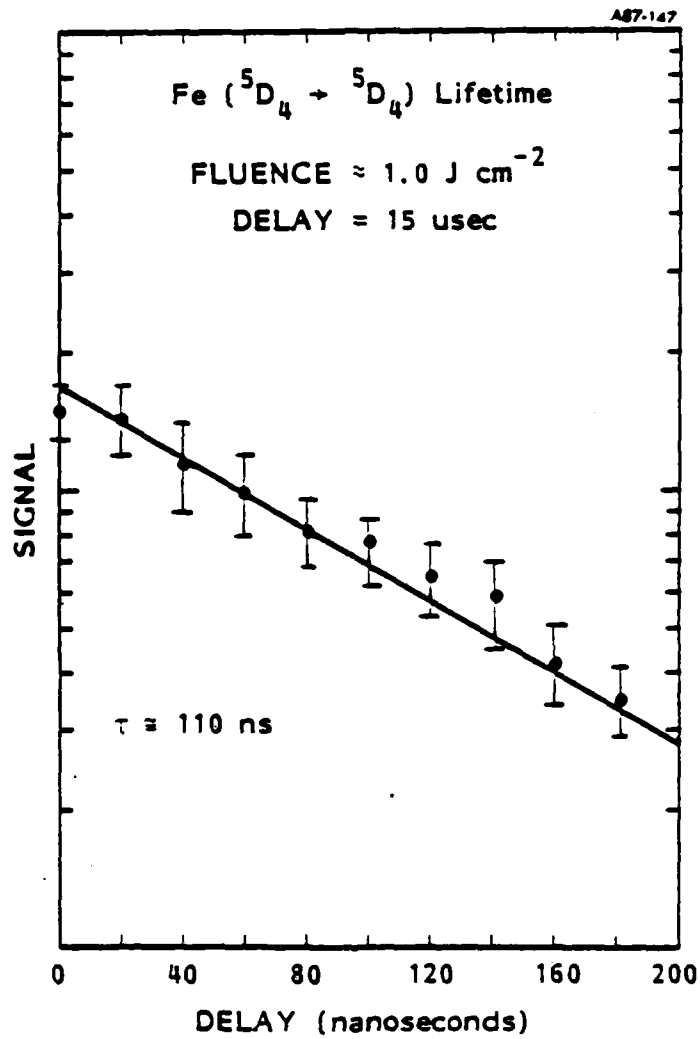
Figure 3. Fluorescence Lifetime Measurement of Atomic Iron Excited at 3859.91 Å
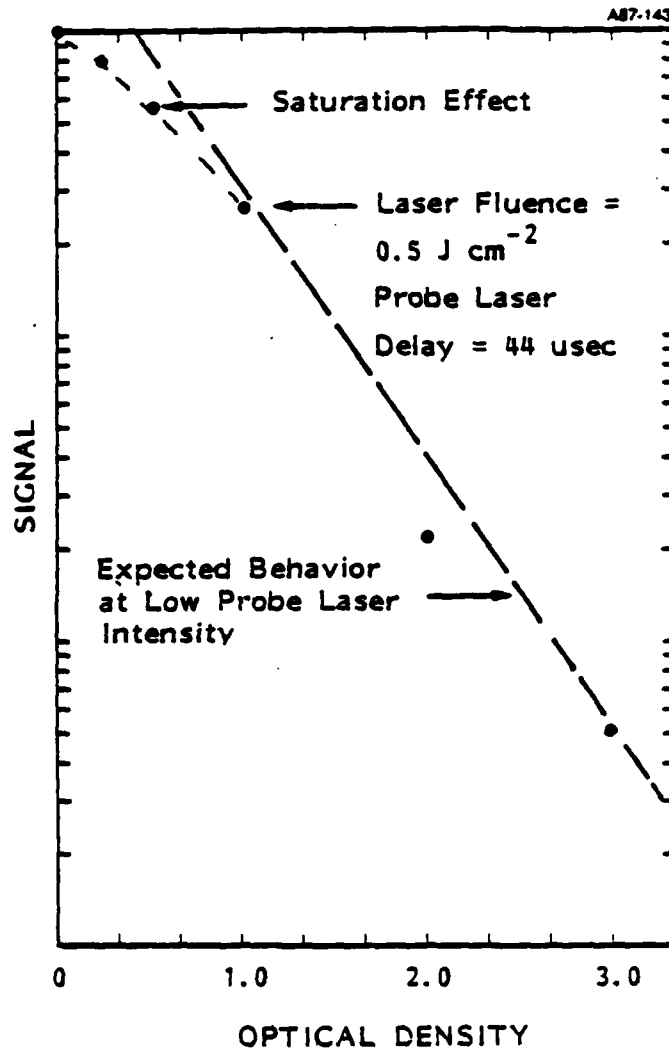
Figure 4. Probe Laser Saturation Measurement. Note that at high laser intensity (low optical depth) the fluorescence signal no longer scales linearly with laser intensity.
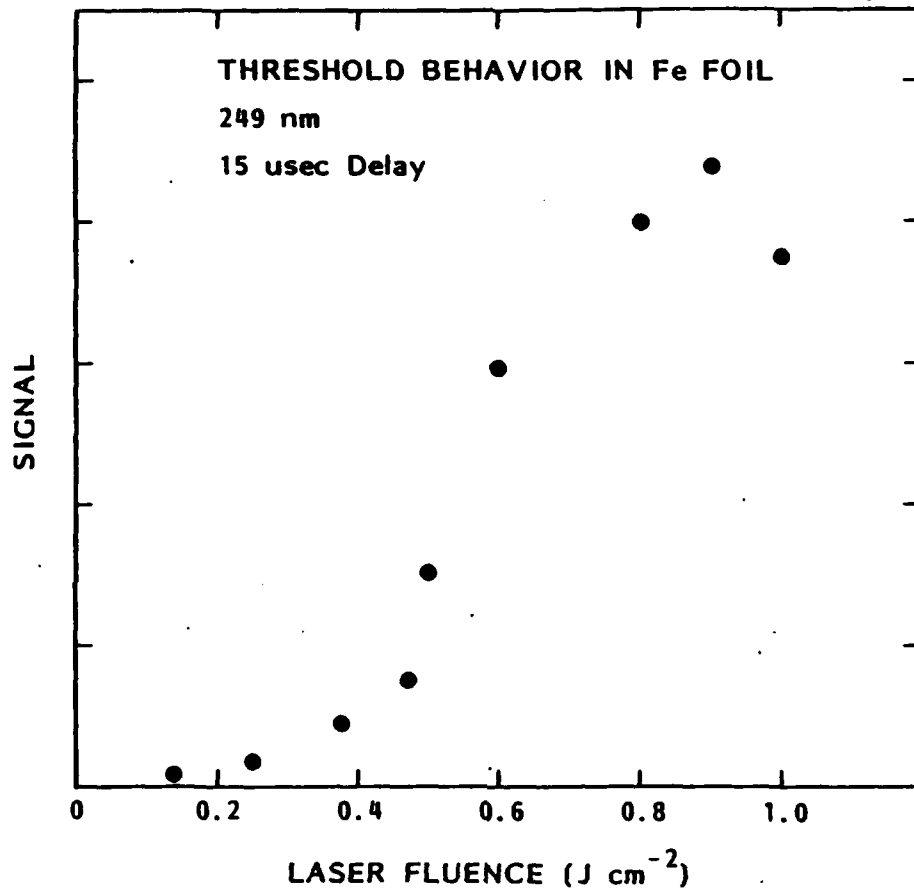
Figure 5. Threshold Measurement. Iron atom induced fluorescence is measured as a function of incident vaporization laser fluence.

fixed set of conditions. A threshold of approximately 0.5 J cm^{-2} is found; negligible signal is measured below 0.1 J cm^{-2}. Accompanying this threshold is a visible plume fluorescence which at short delay times interferes with detecting the induced fluorescence.

In order to set the optimum delay times between the vaporization and probe lasers, the particle velocity distribution was measured. This was done by measuring the time-of-flight spectrum obtained by varying the delay time between the vaporization laser and dye laser and measuring the induced fluorescence at a point two centimeters away from the sample surface.

The velocity flux distribution is related to the time-of-flight distribution by:[12]

$$I(v) = S(t) \frac{L}{t} J(v,t)$$

where L is the flight distance, S(t) is the measured signal, and J is the Jacobian relating time and velocity space:

$$J(v, t) = \left|\frac{dt}{dv}\right| = \frac{t^2}{L} \quad .$$

The extra factor of L/t reflects the fact that induced fluorescence is a measure of number density and must be multiplied by the molecular velocity (L/t) to create a flux density. Figure 6 and 7 show flux distributions at two different laser fluences, one at threshold, the other at a high fluence. They are similar in that they peak at low velocities (below 2 km s^{-1}), but at the higher fluence, a high velocity component becomes more noticeable. The most important finding of this measurement is that the plume is quite spread out in time, with measurable signal out to a 300 μsec delay (!). This indicates that one would prefer to minimize flight distance before detection to insure maximum spatial and temporal overlap between the plume and probe laser beam.
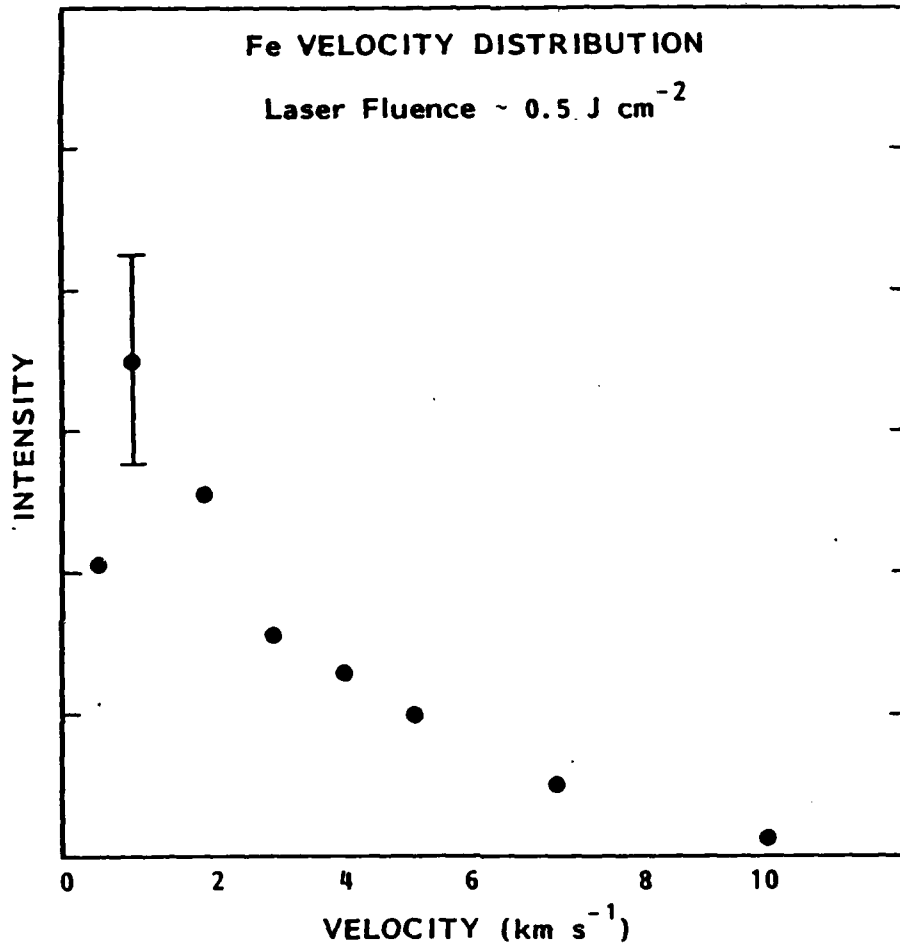
Fe VELOCITY DISTRIBUTION

Laser Fluence ~ 0.5 J cm^{-2}

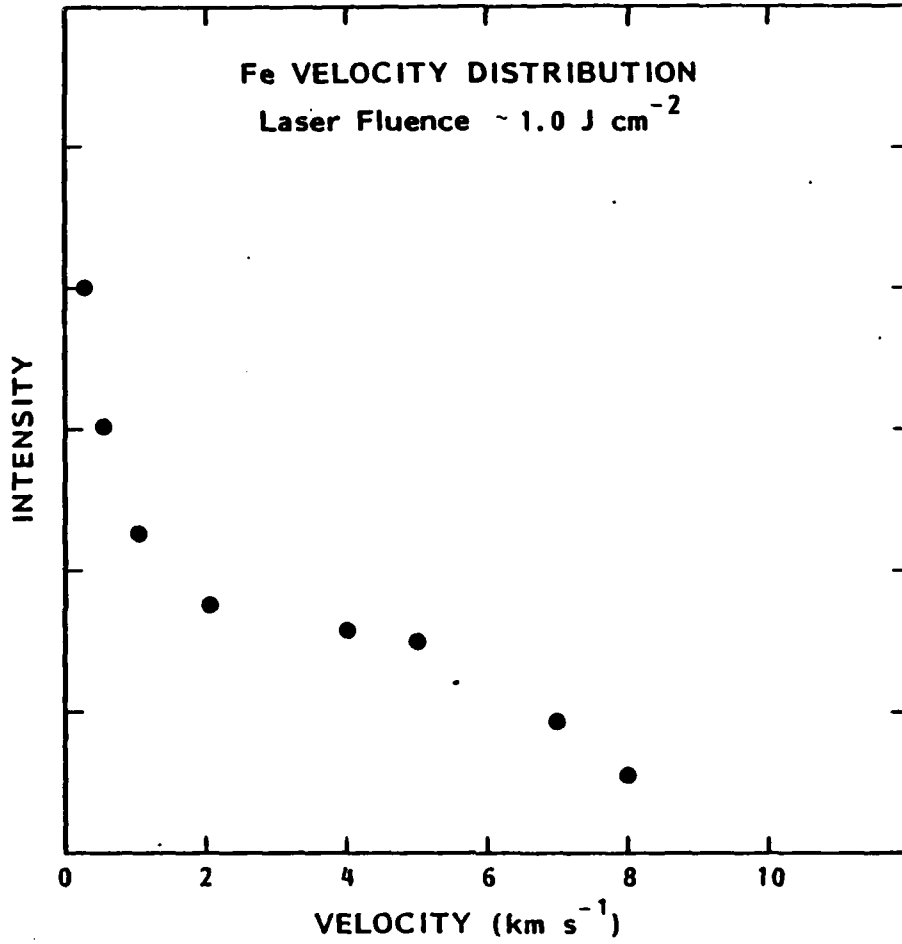Figure 6. Flux Velocity Distribution of Iron Atom Plume at Incident Laser Power of 0.5 J cm^{-2}

Figure 7. Flux Velocity Distribution of Iron Atom Plume at Incident Laser Power of 1.0 J cm^{-2}

3.2 Indium in GaAs

Having investigated the qualities of PALAS on a pure iron foil, we
attempted to measure a concentration profile in a GaAs boule which had been
doped with a few parts per thousand indium. A flat section of the boule was
cut off using a diamond edged saw and used without further preparation (e.g.,
polishing or annealing). An interference filter peaked at 405 nm was used to
lessen background light from the plume. A vaporization laser fluence of 0.6 J
cm^{-2} was used to create the plume. Figures 8 and 9 show induced fluorescence
excitation spectra for both gallium and indium respectively at 4022 Å and 4092
Å at 7 μsec delay between the two lasers. The measured linewidth in both
cases is limited by the spectral resolution of the dye laser.

Having shown that it was trivial to resolve spectral peaks 70 Å apart, we
attempted to measure a profile of the indium concentration by rastering the
vaporization laser across the sample face, pausing at each spot for 200 laser
pulses, half with the probe laser inducing fluorescence and half with the
probe laser blocked. The difference signal represents the contribution from
the induced fluorescence after the plume emission has been subtracted.
Figure 10 shows the average of two scans. While indium is measured with a
signal-to-noise ratio of only two, it is quite apparent when none is present
at the edge of the sample. Furthermore, it appears that the concentration
gradient is positive from left to right before dropping off. There are two
reasons for the scatter in the data. The foremost reason is that in this
case, plume emission from a major species, gallium, can be transmitted through
the interference filter. Even though a difference signal is used to calculate
the indium concentration, the signal from the plume is large enough to almost
swamp the photomultiplier, making this subtraction difficult. A second
problem is that in using 200 laser pulses at each spot and then repeating the
measurement, we are in effect performing a depth profile as well. There was
some indication that each scan gave different results although the poor
statistics preclude any meaningful conclusion.

Visual inspection of the vaporized areas (shown in Figure 11) indicated some melting where 1000 or more laser pulses had irradiated to the area. The oval shape reflects the slight underfilling of the limiting circular aperture by the rectangular laser beam. Measurement of the depth using an optical microscope indicated a range between 0.7 μm and 4 μm, depending on the total number of laser pulses. We estimate that at 0.6 J cm^{-2} fluence, approximately 20-40 Å of gallium arsenide was vaporized per pulse.
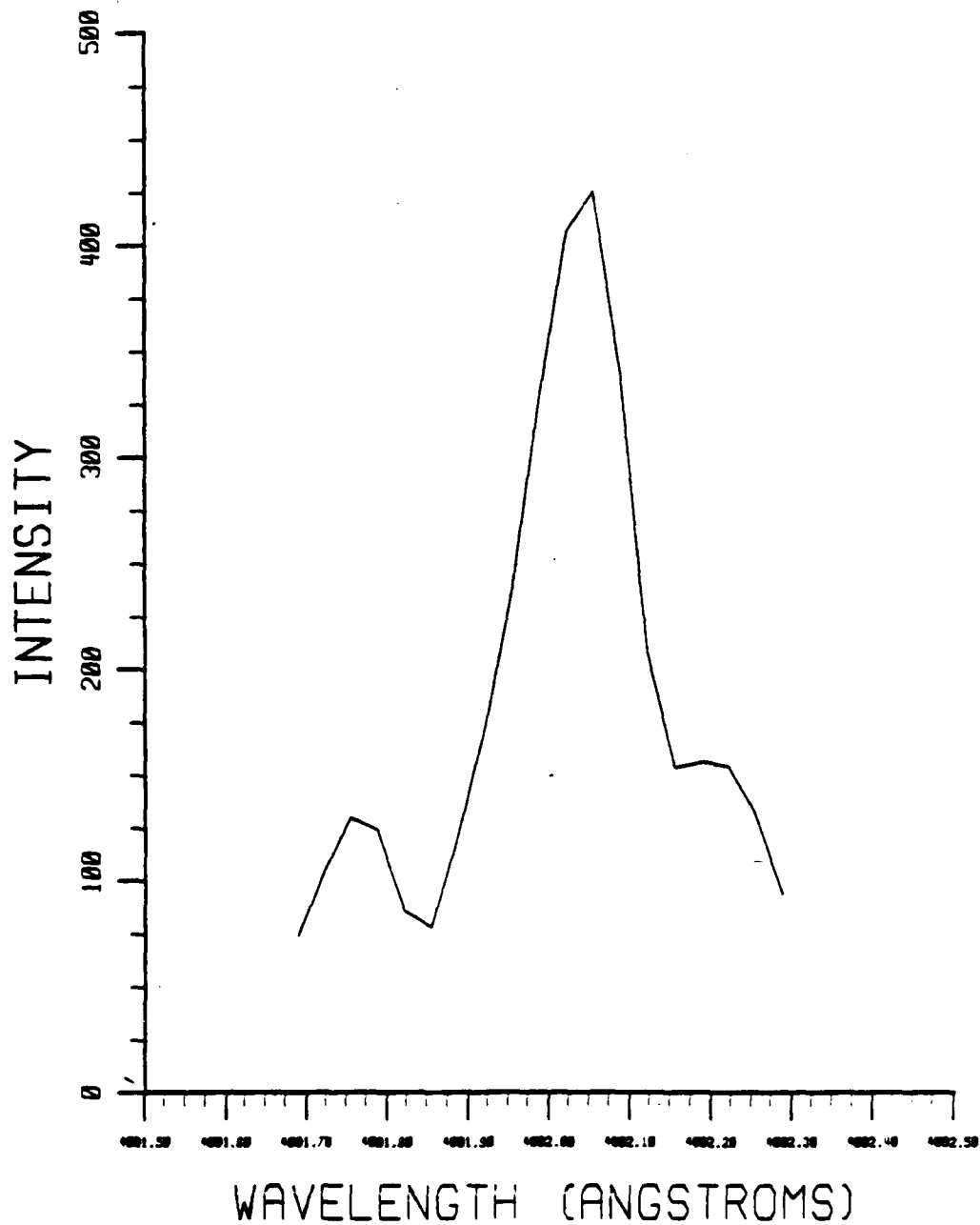
IN EXCITATION SPECTRUM

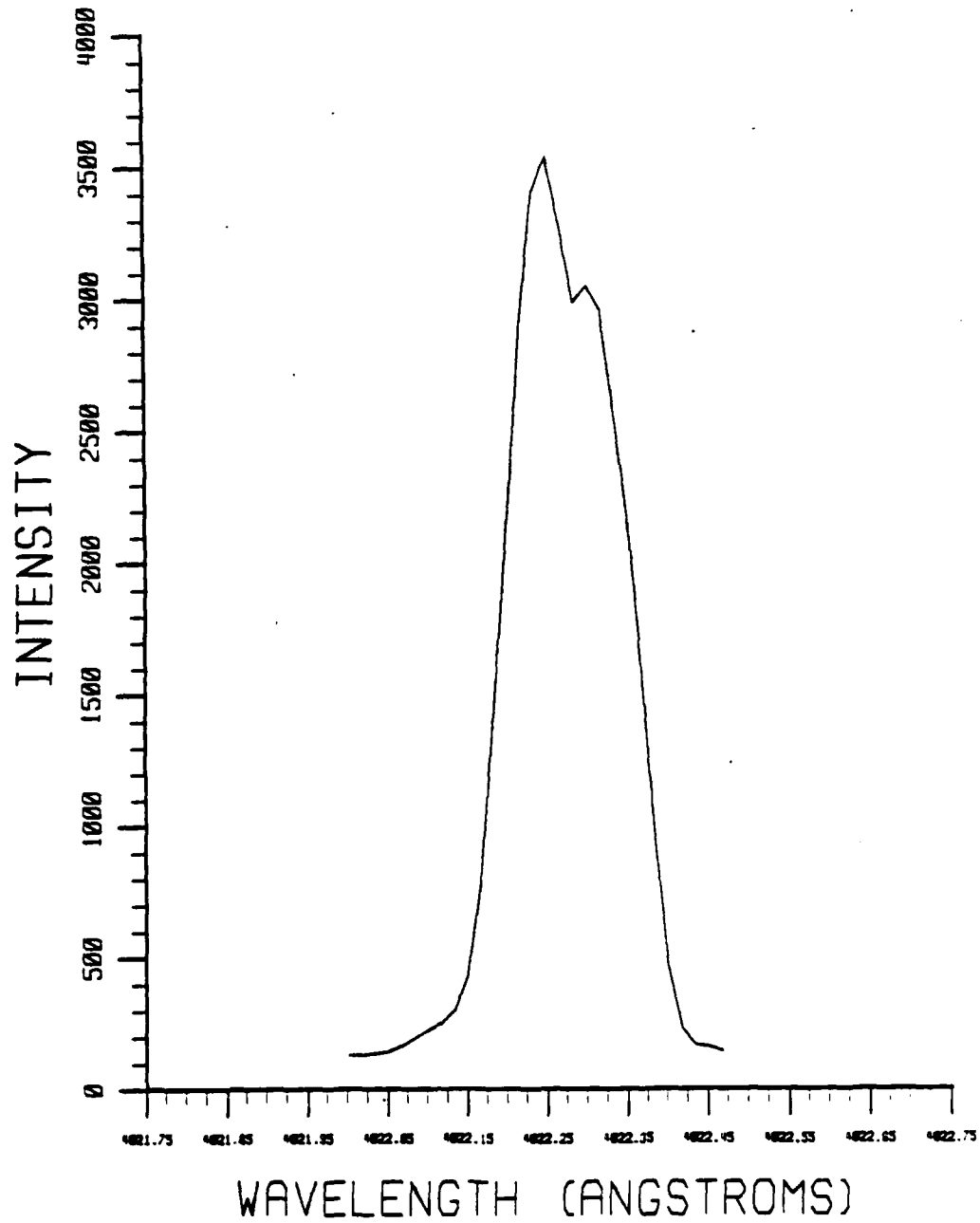Figure 8.   Excitation Spectrum of Indium Vaporized From Gallium Arsenide

GA EXCITATION SPECTRUM

Figure 9. Excitation Spectrum of Gallium Vaporized From Gallium Arsenide

3-13

TRACE ELEMENT INTENSITY PROFILE

Laser Fluence ~ 0.6 J cm^{-2}
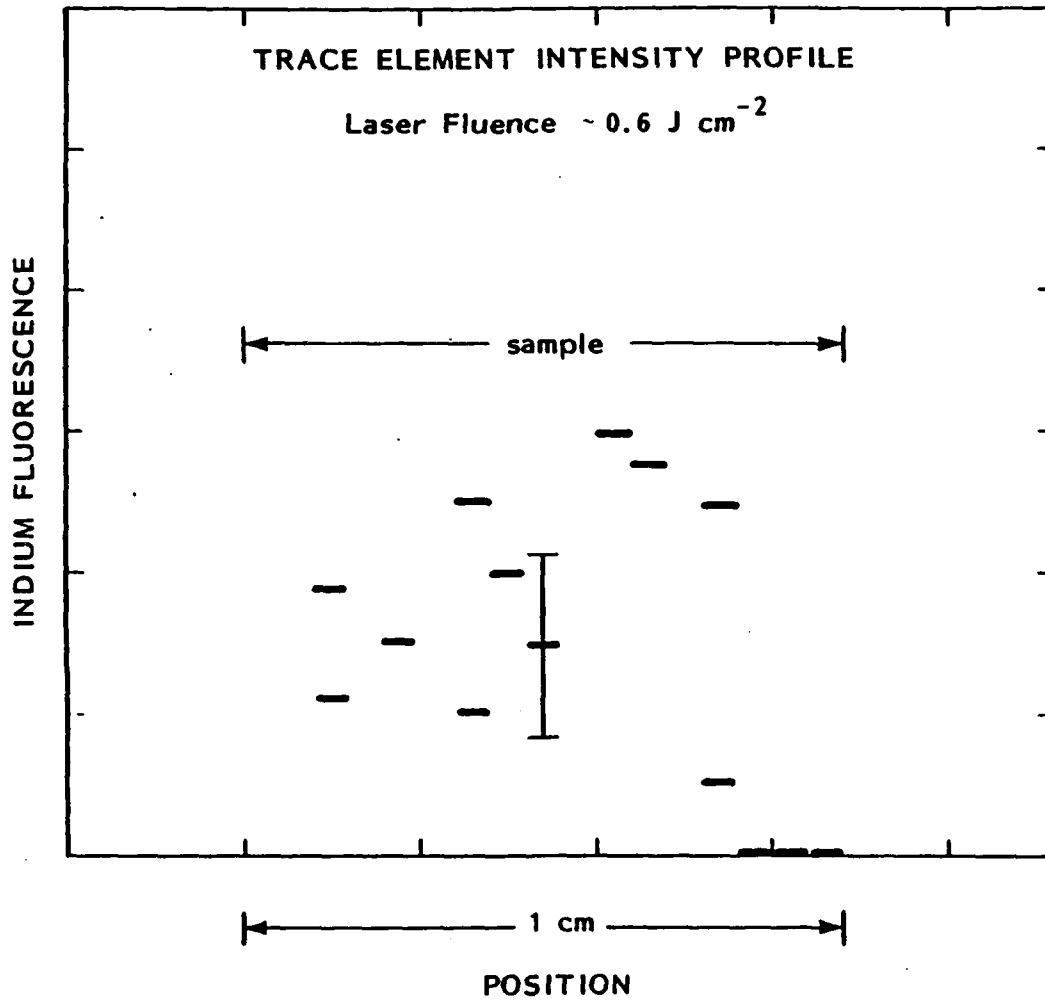
INDIUM FLUORESCENCE

sample

1 cm

POSITION

Figure 10. Composition Profile of Indium Across Gallium Arsenide Sample
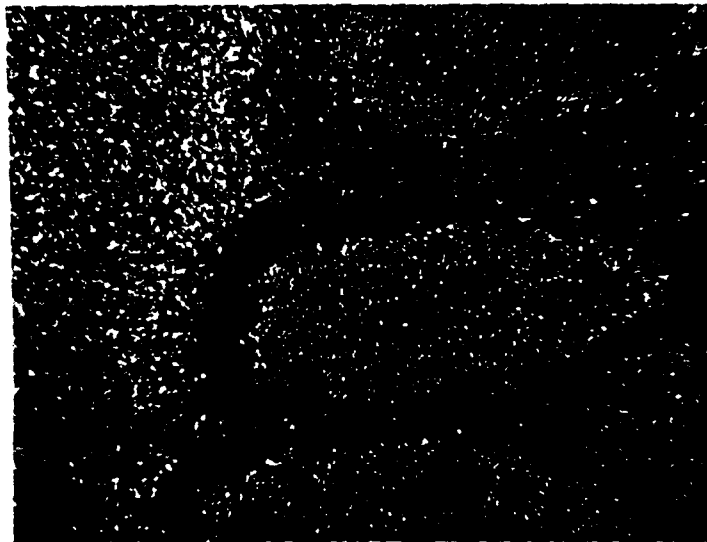
Figure 11. Photograph of Vaporized Sample at Two Magnifications. Etched areas are approximately 0.3 by 0.9 mm in length.

4.0 DISCUSSION

We have been able to show that PALAS provides:

- Unambiguous elemental analysis

- Spatial composition information

- In situ diagnostic capability

at the part per thousand concentration level in semiconductor materials.
Further evidence of the efficacy of this approach to the analysis of
semiconductor materials is provided by work at IBM[13]-[15] on the photoablation
properties of aluminum oxide and polyimide films; their findings on laser
fluence thresholds and particle velocity distributions are similar in nature
to the results reported here. Of course, the pioneering work of Measures and
Kwong[16]-[19] has already established that part per million concentrations are
detectable for metal atoms embedded in composite matrices. (It is unfortunate
that their results on the apparent radiative lifetimes, which are crucial to
understanding plume formation dynamics, have generally been ignored).

Our original proposal stated that sub-part per billion sensitivity might
be possible. The experiments in this report, especially the threshold
results, indicate that this was overly optimistic. In order to obtain enough
vaporized material, we assumed that 1 cm^2 could be vaporized using reasonable
powers. Given our measured threshold requirement of approximately 0.5 J cm^{-2},
this would require a vaporization laser capable of providing five times the
fluence of our present excimer. Furthermore, the plume emission would be so
large as to make any measurement quite difficult. A useful tradeoff, as
presented in the introduction to this report, is to concentrate on spatial
information with a concomitant decrease in sensitivity. Low divergence pulsed
lasers can be focussed to 5 μm spot sizes; the estimates in Table 1 reflect
this and should be reasonable. Depth profiling capabilities should also be

feasible. Evidence suggests that only 5-10 monolayers of material are removed per laser pulse near threshold. Thus, one should be able to profile thin films on binary layered structures quite readily.

As mentioned previously, the major improvement needed in the PALAS system is an improved light discrimination system. The medium band (10 nm) interference filters used in these experiments proved to have too wide a spectral throughput range and too low a broadband blocking effect (10^{-3}). The latter problem reflects the broadband emission that results from the excited atoms and molecules in the hot plume. The filter cannot block enough of the light to prevent the photomultiplier tube from being overwhelmed with signal, causing a very noisy signal even microseconds later. This problem is exacerbated when, as in the case of the indium dopant in gallium arsenide, a major constituent of the plume has a resonant transition close in wavelength to the trace element one is trying to observe. The filter does not discriminate against this emission at all causing even more serious problems. The obvious answer to this is the use of a monochromator which can have far greater resolution, even up to the spectral width of the transition itself. There is a tradeoff between the resolution and signal throughput which must be investigated before the optimum compromise can be reached.

A second improvement involves scattered light from the probe laser which at low signal levels can become the limiting noise factor. In these experiments, the laser light was brought to the apparatus using a fiber optic whose output had to pass through three lenses, a polarizing filter, and an input window before it reached the sample. All these surfaces provide sources of stray light. Therefore, bringing the fiber optic directly into the vacuum chamber where it can be used with only one focusing lens and extensive baffling should greatly reduce the amount of stray light as well as increase the probe laser intensity.

Another major improvement in the system that was not addressed in previous sections would be the inclusion of a turbomolecular pumping system as a replacement for the cryogenically cooled sorption pump. The latter has very

low pumping speed and therefore makes rapid sample cycling difficult. Furthermore, it was apparent that the sorbent material became contaminated from either water vapor and/or substrate material (As, P, etc.) which limited the ultimate obtainable pressure. Frequent replacement of the sorbent became necessary. A turbomolecular pump provides a clean, fast (150 ℓs^{-1}), and easily cyclable pumping system which should be able to provide a vacuum below 10^{-6} torr. At this pressure, interactions between the sample surface and any residual gaseous background become minimal, thereby reducing the possibility of oxide and/or nitride formation during the analysis. Formation of these surface layers can change the vaporization kinetics of the sample, introducing error into any quantitative analysis. We note that standard chemical vapor deposition apparatuses already use turbomolecular pumps to insure system cleanliness and integrity.

In conclusion, we feel that PALAS, although perhaps not a universal tool for quantitative analysis, can provide a comparatively inexpensive approach to the measurement of surface concentrations as well as bulk material depth profiles with specific identification of the species. With the use of fiber optics and compact lasers, it is conceivable that the technique could be directly incorporated into deposition apparatuses.

5. REFERENCES

1. E. Zinner, J. Electrochem. Soc. 130, 199C (1983).

2. W.H. Christie, D.H. Smith, R.E. Eby, and J.A. Carter, Amer. Lab., 19-29, March, 1978.

3. M.A. Rudat and G.H. Morrison, Anal. Chem. 51, 1179 (1979).

4. S. Hoffman, Appl. Phys. 9, 59 (1976).

5. S.C. Yang, A. Freedman, M. Kawaskai, and R. Bersohn, J. Chem, Phys. 72, 1028 (1980).

6. J.A. Silver, D. Worsnop, A. Freedman, and C.E. Kolb, J. Chem. Phys. (accepted for publication).

7. J. Wormhoudt, A.C. Stanton, and J. Silver, Proc. SPIE 452, 88 (1983).

8. W.L. Weise and G.A. Martin, "Transitions Probabilities for Atoms and Atomic Ions", National Bureau of Standards, NSRDS-NBS68 (December 1980).

9. W.L. Weise, M.W. Smith, and B.M. Miles, "Atomic Transition Probabilities", NSRDS-NBS22 (October 1969).

10. H. Okabe, Photochemistry of Small Molecules, Wiley Interscience, New York (1978).

11. C. Gozewski, and J. Silver "Laser Induced Fluorescence Data Acquisition Controller", (ARI-RR-430, 1980).

12. G.E. Busch and K.R. Wilson, J. Chem. Phys. 56, 3636 (1972).

13. R.W. Dreyfus, R. Kelly, and R.E. Walkup, Appl Phys. Lett 49, 1478 (1986).

14. R. Srinivasan, B. Braren, and R.W. Dreyfus, J. Appl. Phys. 61, 372 (1987).

15. R.W. Dreyfus, J.M. Jasinski, G.S. Selwyn, and R.E. Walkup, Laser Focus, p. 62, December 1986.

16. R.N. Measures, N. Drewell, and H.S. Kwong, Phys. Rev. A 16, 1093 (1977).

17. H.S. Kwong and R. Measures, Anal. Chem. 51, 428 (1979).

18. R.M. Measures and H.S. Kwong, Appl. Opt., 18, 281 (1979).

19. H.S. Kwong and R.M Measures, Appl. Opt. 19, 1025 (1980).

MISSION

of

Rome Air Development Center

RADC plans and executes research, development, test and selected acquisition programs in support of Command, Control, Communications and Intelligence (C³I) activities. Technical and engineering support within areas of competence is provided to ESD Program Offices (POs) and other ESD elements to perform effective acquisition of C³I systems. The areas of technical competence include communications, command and control, battle management information processing, surveillance sensors, intelligence data collection and handling, solid state sciences, electromagnetics, and propagation, and electronic reliability/maintainability and compatibility.